

# Predictability of the coupled troposphere-stratosphere system

**Heiner Körnich**

*Department of Meteorology, Stockholm University*  
*Stockholm, Sweden*  
[heiner@misu.su.se](mailto:heiner@misu.su.se)

## **Abstract**

Tropospheric predictability is typically limited to about 20 days due to the chaotic nature of weather. The tropospheric variability contains planetary waves which can propagate vertically into the winter stratosphere, where they break and drive a residual meridional circulation. For cases of exceptionally strong planetary wave activity, this circulation can induce a polar stratospheric warming and a subsequent downward propagation of the circulation anomaly to the troposphere. This process provides an increased predictability for the troposphere. The predictability is associated with the zonal mean zonal wind around 60°N and the Northern Annular Mode, which tends to a negative phase after a stratospheric warming event. The negative Northern Annular Mode phase yields colder temperatures in Mid- and Northern Europe. Thus, the coupled troposphere-stratosphere system improves tropospheric predictability on monthly to seasonal time-scales. This article reviews briefly the observed phenomena, the current theoretical understanding, and the role for numerical weather prediction.

## **1. Introduction**

The role of the stratosphere for numerical weather prediction has long been underestimated, commonly referring to the small mass, only about 25% of the total atmosphere, as the tail does not wag the dog. This fact is reflected in the commonly low lid of forecast models around 10 hPa. Dynamical influence was regarded to propagate bottom-up, as it is known of planetary, gravity, and tidal waves. Recent work has stressed the top-down influence of the stratosphere on the troposphere, which will be reviewed in the following.

## **2. The observed troposphere-stratosphere coupling**

The stratospheric impact on tropospheric dynamics is often paraphrased with the so-called "downward propagation" of zonal wind anomalies (Baldwin and Dunkerton, 2001). The wind anomalies are expressed in terms of the Northern Annular Mode (NAM), which describes a seesaw of geopotential anomalies between high and mid-latitudes. Baldwin and Dunkerton (2001) defined weak and strong stratospheric vortex events, if the index of the normalized 10-hPa NAM crosses -3.0 and +1.5, respectively. Weak vortex events are accompanied by a warming of the polar stratosphere, so-called stratospheric warmings. The circulation anomaly during the events propagates downward from 10 hPa to the tropopause within about a week. The following 60 to 80 days display a significant NAM anomaly in the troposphere with the same sign as the previous stratospheric anomaly. The surface pressure anomaly in response to the troposphere and stratosphere coupling resembles a negative (positive) North Atlantic Oscillation (NAO) pattern for the weak (strong) vortex regimes.

The downward propagation was reproduced by creating a mean time-lagged composite for major stratospheric warming events in ECMWF's ERA interim data from 1989 to 2010 (Fig.1). The central date of the warming events is defined by the first day when the zonal mean zonal wind at 10hPa and 60°N becomes negative during NH winter. Final warmings have been excluded. Figure 1 shows the composite of the 00UTC zonal mean zonal wind anomalies at 60°N before and after the central date. The anomaly is achieved by removing the smoothed daily climatology from 1989 to 2010 from ERA interim. The downward propagation of the negative zonal wind anomalies is clearly visible in the stratosphere. Furthermore, the troposphere displays a tendency towards negative zonal wind anomalies after the warming.

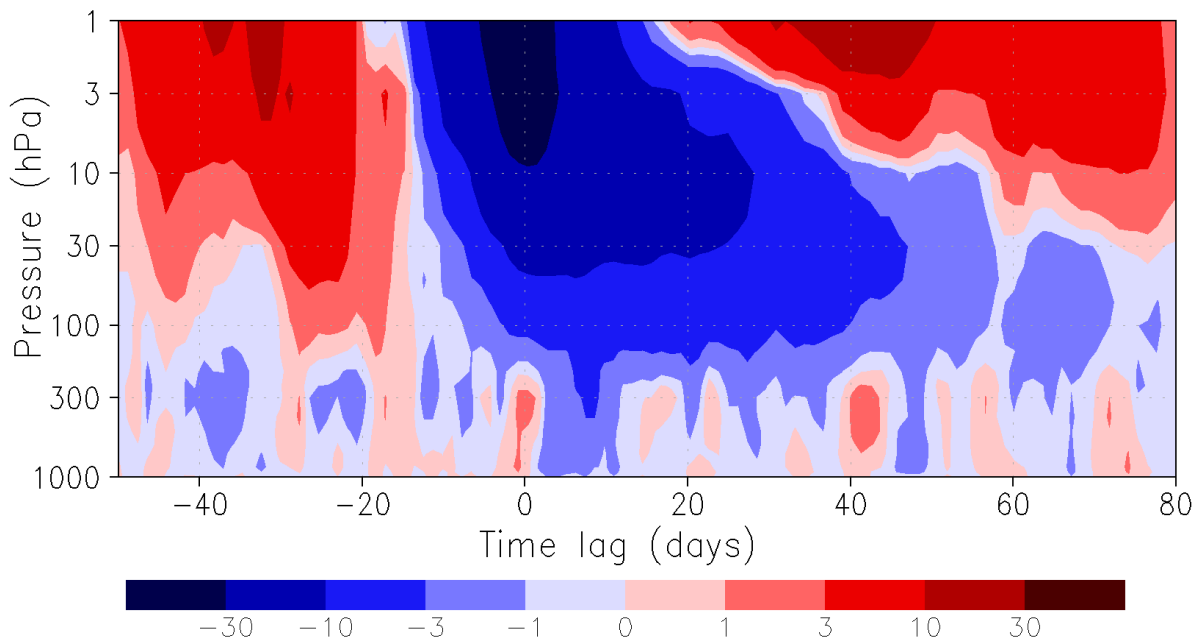


*Figure 1: Composite of zonal mean zonal wind anomaly ( $ms^{-1}$ ) at 60°N for major stratospheric warming events from 1989 to 2010 in ERA interim data. The anomaly is achieved by removing the smoothed daily climatology calculated over the entire time series.*

A specific example of the downward influence was presented for the winter 2005/2006 by Scaife and Knight (2008). A strong stratospheric warming occurred in January 2006. During the following month, Europe was under cold spell with low NAO index values. Central England and Northern European experienced low temperatures and weak zonal winds.

The general surface response to anomalies in the stratospheric vortex was shown by Thompson et al. (2002). Composites anomalies for weak and strong vortex conditions at 10 hPa were averaged over following 60 days after the onset of the stratospheric anomaly. The difference between weak and strong vortex cases shows that a general cooling of up to 4 K over Eurasian middle to high latitudes.

Figure 2 shows the 2-metre temperature anomaly following days 1 to 60 after the major stratospheric warming based from ERA interim data. Although temperatures are not as low as in Thompson et al. (2002), the pattern of cold North-Western America and Northern Europe is clearly reproduced. Interestingly, the 2-metre temperature plays a positive anomaly over North-East America and Central Asia.

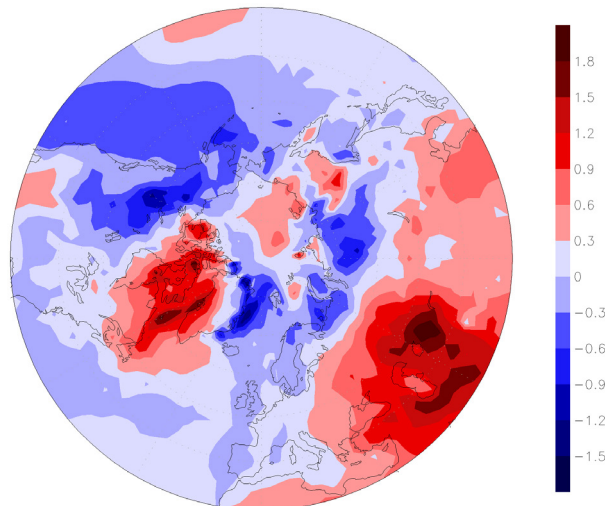


Figure 2: Composite of daily mean surface temperature anomalies for the 60-day interval following the major stratospheric warming events of 1989 to 2010 from ERA interim.

The active phase of the troposphere-stratosphere coupling is restricted to the stratospheric winter, as only the stratospheric westerlies in winter allow for vertical propagation of planetary waves which are the decisive player for the coupling process. Gerber et al. (2010) showed from reanalysis that the NAM displays strong variance during boreal winter from December to March, while the stratospheric southern annular mode has most variance towards the end of the winter (September to December). The difference results from the fact that planetary waves are usually stronger in the Northern Hemisphere due to stronger topography and land-sea contrasts leading to generally weakened stratospheric westerlies. The stratospheric vortex in the Southern Hemisphere is characterized by its stability in mid-winter being variable only at the end of the winter.

Another coupling of tropospheric and stratospheric dynamics is manifested in the correlation between tropospheric and stratospheric geopotential height fields (Perlwitz and Harnik, 2004). The zonal mean component clearly reproduces the downward propagation as described above. Furthermore, Perlwitz and Harnik (2004) stressed the lagged correlation for the wave component. Maximum correlation is achieved when the tropospheric geopotential wave leads the stratosphere by about five days which is consistent with the upward propagation of tropospheric waves. However a secondary maximum occurs when the stratospheric geopotential leads the tropospheric one at a time lag of about eight days. It is further demonstrated that this secondary maximum results from planetary waves which were reflected downwards in the stratosphere.

In summary, stratospheric circulation anomalies have been observed to affect surface climate via the NAM pattern. A further process for troposphere-stratosphere coupling is the downward reflection of vertically propagating planetary waves.

### 3. Mechanisms for troposphere-stratosphere coupling

The basic theory for stratospheric warmings was presented by Matsuno (1971). Increased planetary wave activity flux (Eliassen-Palm flux) propagates from the troposphere upwards. After preconditioning the polar vortex the breaking of the waves takes place in high latitudes of the stratosphere. The induced wave drag gives rise to a stronger residual circulation accompanied with a

strong polar warming. The change in the meridional temperature gradient creates stratospheric easterlies. Subsequent planetary wave activity will break at lower altitudes as the easterlies prevent a higher propagation. The stratospheric downward propagation was visualised by Christiansen (1999) in a simple model.

For the tropospheric response to the stratospheric anomaly two different ideas are discussed recently, the balanced response and the response mediated by baroclinic waves.

The balanced wind response was analysed by Thompson et al. (2006) based on the quasi-geostrophic equations in the transformed Eulerian mean. Equivalent to this balanced wind response are formulations using potential vorticity inversion (Black, 2002; Ambaum and Hoskins, 2002). In the balanced wind response, the driving forces for the residual meridional circulation are, on the one hand, the wave drag (Eliassen-Palm flux divergence) and the friction in the zonal momentum equation, and on the other, the diabatic heating in the thermodynamic equation. Interestingly the two driving forces generate zonal wind with a characteristic difference in the vertical structure. Let us have a closer look at the zonal wind response in high latitudes around  $60^\circ$  latitude (Thompson et al. 2006, their Fig. 3). The stratospheric wave drag strengthens the meridional overturning circulation, i.e. the residual circulation, with stronger downwelling in high latitudes. This increases temperatures in the polar stratosphere and weakens the zonal component of the thermal wind. At the surface the southward flow of the residual circulation gives rise to an eastward Coriolis force with anomalous eastward flow which is balanced by surface friction. Thus, both surface and stratosphere experience a negative zonal wind anomaly. For diabatic heating forcing, the stratospheric high latitude cooling

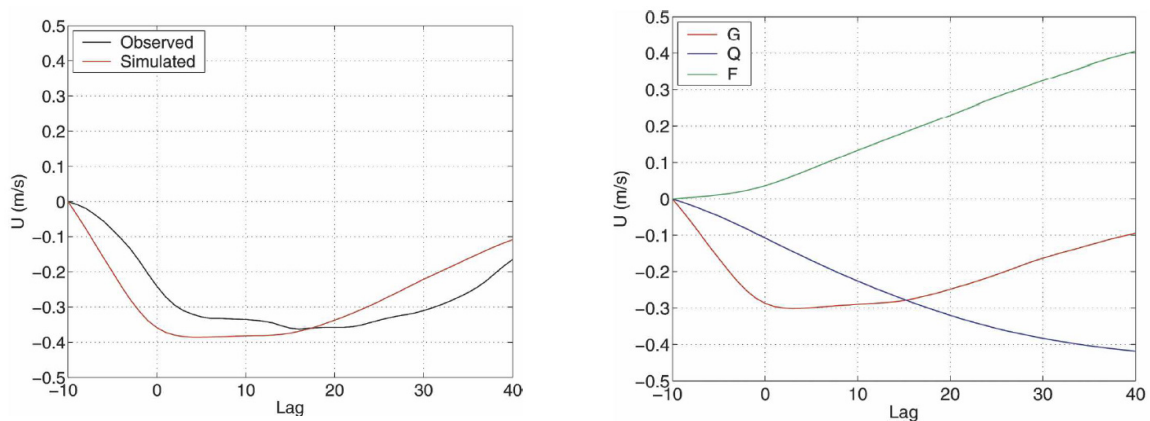


Figure 3: (Left) The time-integrated response of the zonal-mean zonal wind averaged over  $55^\circ$ – $75^\circ$ N at 925 hPa to stratospheric wave drag  $G$  (red), surface friction  $F$  (green), and stratospheric diabatic cooling  $Q$  (blue). (Right) The total simulated balanced wind response (red) and the corresponding observed zonal-mean zonal wind anomalies (black). All wind anomalies are shown with respect to their values at day -10.  
 (Figure and adjusted caption taken from Thompson et al. 2006, their Fig. 7)

© Copyright 2006 American Meteorological Society (AMS). Permission to use figures, tables, and brief excerpts from this work in scientific and educational works is hereby granted provided that the source is acknowledged. Any use of material in this work that is determined to be "fair use" under Section 107 or that satisfies the conditions specified in Section 108 of the U.S. Copyright Law (17 USC, as revised by P.L. 94-553) does not require the Society's permission. Republication, systematic reproduction, posting in electronic form on servers, or other uses of this material, except as exempted by the above statements, requires written permission or license from the AMS. Additional details are provided in the AMS Copyright Policies, available from the AMS at 617-227-2425 or [amspubs@ametsoc.org](mailto:amspubs@ametsoc.org).

drives a stronger residual circulation with the same consequences for the surface winds, i.e. a negative zonal wind anomaly. However in the stratosphere the polar cooling results in a strengthening of the zonal component of the thermal wind. The zonal wind anomalies for diabatic heating are in opposite directions in the stratosphere and the surface.

The transfer of the above considerations to a stratospheric warming event leads to the following balanced wind response at the surface. For this purpose, Thompson et al. (2006) applied the lag regression of the inverted 10-hPa NAM index on different fields of the ERA-40 reanalysis. This usage of the inverted NAM index makes the results comparable to the development of a stratospheric warming with a weakening of the stratospheric jet. From the onset stage of the warming from day -10 to +15, the zonal wind change at the surface around 60° latitude are dominated by the response to the increased stratospheric wave drag (right panel in Fig. 3). The increased stratospheric temperature in high latitudes induces a stronger radiative cooling which dominates the zonal wind response at the surface in the later stage of a warming from day 15 onwards (right panel in Fig. 3). When also adding the surface friction to these two balanced wind responses by wave drag and radiative cooling, a reasonable reproduction of observed zonal wind responses is achieved (left panel in Fig. 3). However, it should be noted that the balanced wind response for lags larger than 20 days underestimates the observations by about 20%.

An alternative idea involves the response of tropospheric baroclinic eddies to stratospheric circulation anomalies. Kunz et al. (2009) separated anticyclonic and cyclonic wavebreaking events on the North Atlantic based on ERA-40 reanalysis. Zonal wind anomalies in the upper troposphere resemble a positive (negative) NAM response for the anticyclonic (cyclonic) wavebreaking. Furthermore it was demonstrated that cyclonic wavebreaking dominates during 20 to 30 days after a stratospheric warming event. This difference in wavebreaking can be understood by analysing a modified Eady problem in an idealised general circulation model (Wittmann et al. 2007). These experiments are initialised with a prescribed zonal wind jet. The jets in the experiments differ in the vertical gradient at the tropopause, ranging from a negative over a neutral to a positive gradient. Nonlinear life cycle calculations confirmed analytical solutions from a linear model. For low zonal wave numbers, the growth rate increases with the shear at the tropopause, while the growth rates for higher zonal wave numbers decreases with the shear. This means that for a stratospheric warming event with negative zonal wind shear at the tropopause, baroclinic eddies with higher zonal wave numbers will occur more frequently. Additionally the nonlinear calculations demonstrated a transition from anticyclonic to cyclonic wavebreaking at those higher zonal wave numbers, i.e. zonal wave number 7. Thus, the more cyclonic wavebreaking for stratospheric warming events predicted from these nonlinear life cycle calculations are consistent with the observations by Kunz et al. (2009). The cyclonic wavebreaking leads then to a negative NAM anomaly in the troposphere.

Both theories of tropospheric response to stratospheric warmings are likely to be important. As noted above the balanced wind response misses a part of the response at longer timescales.

For the reflection of planetary waves in the stratosphere, Harnik and Lindzen (2001) suggested to separate the classical formulation of the refractive index for Rossby waves into a vertical and meridional component. When focusing on the vertical propagation conditions, it turned out that the vertical shear of the zonal wind provides the most important criterion for vertical propagation. The reanalysis years were then separated according to the zonal wind difference between 2 and 10 hPa,

averaged over 58°N to 74°N. For non-reflective years, stratospheric anomalies in the zonal mean geopotential were leading tropospheric anomalies by about two weeks. So, planetary waves are breaking in the stratosphere, inducing a circulation anomaly which can propagate downwards to the troposphere. For reflective years however, stratospheric anomalies in the eddy geopotential occurred before the tropospheric eddy anomalies. This represents the reflection of planetary waves from the stratosphere downwards. The zonal mean component showed no clear lead-lag behavior in the reflective years.

In summary, tropospheric responses to stratospheric circulation anomalies can be explained either by a balanced wind response following the downward-control principle (Haynes et al. 1991) or by a modified baroclinic eddy response due to the changed vertical zonal wind gradient at the tropopause. Furthermore, the vertical zonal wind gradient in the stratosphere plays an important role for the reflection of planetary waves.

#### **4. Forecasting troposphere-stratosphere coupling**

The forecasting of a stratospheric warming event can generally be separated into two parts: 1) the problem of forecasting the preconditioning and growth of the warming, and 2) the forecast of the maintenance and decay of the warming including its impact on the troposphere. Alternatively, it could be argued that the tropospheric anomaly persists already from the initialisation of the stratospheric warming event.

Knowledge of the stratospheric NAM provides a higher predictability of the monthly mean surface Arctic Oscillation and the usage of the Arctic oscillation itself (Baldwin et al. 2003). This finding was confirmed by Christiansen (2005) who combined a dynamical with a statistical forecast of the surface wind (Fig. 4). The dynamical forecast was provided by a version of the ECMWF model with a model top at 10 hPa. Thus the model contains no complete description of the stratosphere. When adding the 70-hPa zonal wind as a statistical predictor, the overall forecast could be significantly improved on timescales longer than 10 days.

The prediction of stratospheric warmings was examined in different case studies. Two events were analysed by Hirooka et al. (2007). The authors used a one-month ensemble forecast by the Japan Meteorological Agency with a model top at 0.4 hPa. The predictability of the stratospheric event depends on the complexity of the dynamics of circulation. While for a certain event (December 2001) the warming could be predicted 16 days in advance, the predictability decreases to only 9 days for more complex situations (December 2003). Marshall and Scaife (2010) analysed four major warming events with two different versions of the Hadley Centre's atmospheric climate model. While the standard version extends only up to about 3 hPa, the extended version reaches 0.004 hPa with 50% more vertical levels than the standard version. The average lead-time for capturing the warming event increased from 8 days for the standard model to 12 days for the extended model. Furthermore the peak of the stratospheric easterlies during the warming increased from 30% of the observed value in the standard model to 60% in the extended model. These improvements provide a better seasonal prediction skill of the extended model for European winter cold spells following the warming events. The forecast error for stratospheric warmings is dominated by errors in the phase of the planetary waves affecting the forecasted divergence of the Eliassen-Palm flux, i.e. the stratospheric wave drag, while the wave amplitude is captured relatively well (Stan and Straus 2009).

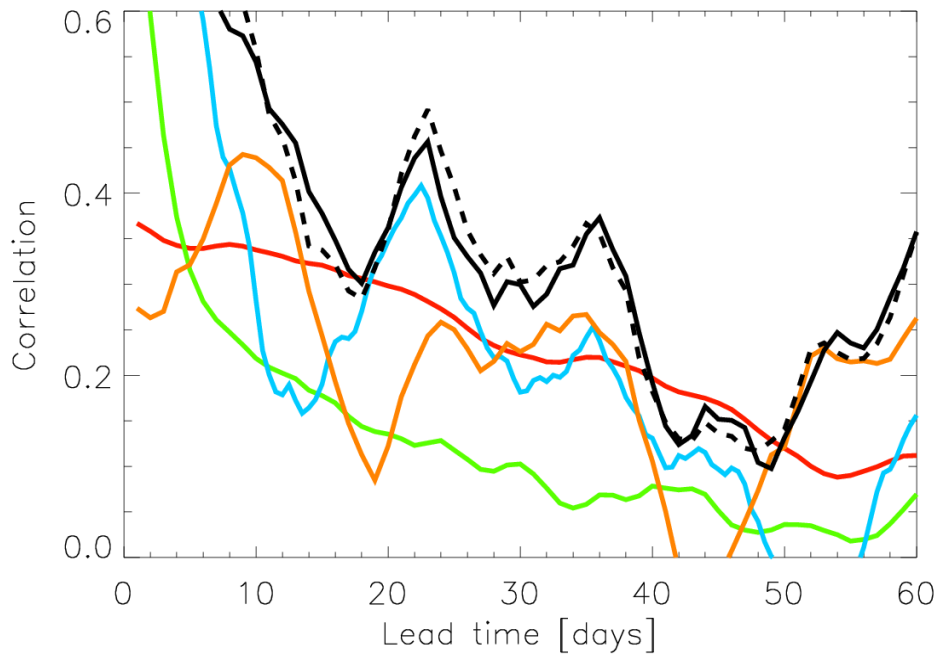


Figure 4: The dynamical ensemble forecast (blue curve) compared to the statistical forecast. The predictand is the surface zonal mean wind at  $60^{\circ}\text{N}$ . The red and green curves are statistical forecasts with the predictor at 1000 hPa and 70 hPa, respectively. The orange curve is a statistical forecast with the predictor at 70 hPa including only the same 51 events as the dynamical ensemble forecast. The full black curve is the combined statistical forecast using both the zonal mean wind at 70 hPa and the dynamical ensemble forecast as predictors. The dashed black curve is the theoretical correlations of the combined forecast if the two predictors were uncorrelated. Taken from Christiansen (2005, his Fig. 9). © Copyright 2005 American Geophysical Union (AGU).

The extension of tropospheric predictability in connection with stratospheric warming events was already demonstrated by Kuroda (2008) using the next-generation seasonal prediction model of the Japan Meteorological Agency. The model extends vertically up to 0.4 hPa (about 55 km) with a spectral resolution T95 (about 200 km grid). Following a stratospheric warming event in January 2004, the predictability of the anomalous zonal mean zonal wind, averaged over  $55$  to  $65^{\circ}\text{N}$ , increased to 2 months in the troposphere and 3 months in the stratosphere. It was demonstrated by Kuroda (2008) that this long forecast skill results to a large extent from the inclusion of a stratosphere in the forecast model. A further important factor was the sea-surface temperature anomaly at the initial time.

Interestingly, the increased predictability showed a high sensitivity to the initial time of the forecast (Kuroda 2010). For initial times of a few days before the warming, the high predictability occurred, but it vanished for initial times shortly after the warming event, although the initial time would be closer to the verification time.

An alternative hypothesis for the predictability assumes the persistence of the tropospheric anomaly. It was tested by Gerber et al. (2009). In an idealized General Circulation Model (GCM) reaching up to 0.7 hPa, the forecast was initialized 10 days before a major warming. The tropospheric state was perturbed in order to destroy coherent structures which could provide persistence. The tropospheric forecast after 40 to 90 days showed a strong negative NAM index for 88 of 100 cases, demonstrating



the stable tropospheric response to the stratospheric warming. This downward propagation to the troposphere was only observed, if the tropospheric NAM is neutral or positive at the first day of the stratospheric warming. Otherwise, the troposphere displays a simultaneous response to the stratospheric circulation anomalies.

The general importance of the stratosphere for tropospheric forecasts was demonstrated by Polavarapu (2010) using the operational forecast model of the Canadian Meteorological Centre for the time span from December 20 to January 26, 2006. The root mean squared error between observed and 5-day forecasted geopotential showed a reduction throughout the troposphere, if the model included a higher top, i.e. a realistic model description of the stratosphere. This reduction was of the same order of magnitude as the improvement, when moving from a 3-d to a 4-d variational data assimilation system. The high-top effect was larger in winter than in summer season and it could be attributed mainly to the model changes, namely the high-top and the improved radiative scheme.

## 5. Conclusions

Tropospheric predictability is typically limited to about 20 days (Bengtsson et al. 2008) due to the chaotic nature of weather. The tropospheric variability contains planetary waves which can propagate vertically into the winter stratosphere, where they break and drive a residual meridional circulation. For cases of exceptionally strong planetary wave activity, this circulation can induce a polar stratospheric warming and a subsequent downward propagation of the circulation anomaly to the troposphere.

The slow downward propagation during stratospheric warming events provides additional predictability for the troposphere of 2 to 3 months. The predictability is associated with the zonal mean zonal wind around 60°N and the Northern Annular Mode, which tends to a negative phase after a stratospheric warming event. The negative Northern Annular Mode phase gives rise to colder temperatures in Mid- and Northern Europe.

In order to benefit from the increased predictability of the coupled troposphere-stratosphere system, the forecast model has to include a realistic representation of stratospheric processes. The main component seems to be a sufficiently high model top, i.e. at least reaching up to the lower mesosphere. This model extension seems to provide an equally large improvement as the migration from 3d- to 4d-variational data assimilation. Thus, the coupled troposphere-stratosphere system provides a useful improvement of tropospheric predictability on monthly to seasonal time-scales.

## References

- Ambaum, M. H. P. and B. J. Hoskins, 2002: The NAO troposphere–stratosphere connection. *J. Climate*, **15**, 1969-1978.
- Baldwin, M.P., and T.J. Dunkerton, 2001: Stratospheric harbingers of anomalous weather regimes. *Science*, **294**, 581-584.
- Baldwin, M.P., D.B. Stephenson, D.W.J. Thompson, T.J. Dunkerton, A.J. Charlton, A. O'Neill, 2003: Stratospheric memory and extended-range weather forecasts, *Science*, **301**, 636-640.
- Bengtsson, L.K, E. Källén, L. Magnusson, 2008: Independent Estimations of the Asymptotic Variability in an Ensemble Forecast System. *Mon. Wea. Rev.*, **136**, 4105-4112.



- Black, R. X., 2002: Stratospheric forcing of surface climate in the Arctic oscillation. *J. Climate*, **15**, 268-277.
- Christiansen, B., 1999: Stratospheric vacillations in a general circulation model, *J. Atmos. Sci.*, **56**, 1858-1872.
- Christiansen, B., 2005: Downward propagation and statistical forecast of the near-surface weather. *J. Geophys. Res.*, **110**, D14104.
- Gerber, E. P., C. Orbe, and L. M. Polvani, 2009: Stratospheric Influence on the Tropospheric Circulation Revealed by Idealized Ensemble Forecasts. *Geophys. Res. Lett.*, **36**, L24801, doi:10.1029/2009GL040913.
- Gerber, E. P., M. P. Baldwin, and CCMVal-2 coauthors, 2010: Stratosphere-Troposphere Coupling and Annular Mode Variability in Chemistry-Climate Models. *J. Geophys. Res.*, **115**, D00M06, doi:10.1029/2009JD013770.
- Harnik, N., and R. S. Lindzen, 2001: The effect of reflecting surfaces on the vertical structure and variability of stratospheric planetary waves. *J. Atmos. Sci.*, **58**, 2872-2894.
- Haynes, P. H., C. J. Marks, M. E. McIntyre, T. G. Shepherd, and K. P. Shine, 1991: On the downward control of extratropical diabatic circulations by eddy-induced mean zonal forces. *J. Atmos. Sci.*, **48**, 651-678.
- Hirooka, T., T. Ichimaru, and H. Mukougawa, 2007: Predictability of stratospheric sudden warmings as inferred from ensemble forecast data: Intercomparison of 2001/02 and 2003/04 winters. *J. Meteor. Soc. Japan*, **85**, 919-925.
- Kuroda, Y., 2008: Role of the stratosphere on the predictability of medium-range weather forecast: A case study of winter 2003–2004. *Geophys. Res. Lett.*, **35**, L19701, doi:10.1029/2008GL034902.
- Kuroda, Y., 2010: High initial-time sensitivity of medium-range forecasting observed for a stratospheric sudden warming. *Geophys. Res. Lett.*, **37**, L16804, doi:10.1029/2010GL044119.
- Kunz, T., K. Fraedrich, and F. Lunkeit, 2009: Impact of synoptic scale wave breaking on the NAO and its connection with the stratosphere in the ERA-40 reanalysis. *J. Climate*, **22**, 5464-5480.
- Marshall, A. G., and A. A. Scaife, 2010: Improved predictability of stratospheric sudden warming events in an atmospheric general circulation model with enhanced stratospheric resolution, *J. Geophys. Res.*, **115**, D16114, doi:10.1029/2009JD012643.
- Matsuno, T., 1971: A dynamical model of the stratospheric sudden warmings. *J. Atmos. Sci.*, **28**, 1479–1494.
- Perlwitz, J., and N. Harnik, 2004: Downward coupling between the stratosphere and troposphere: The relative roles of wave and zonal mean processes. *J. Climate*, **17**, 4902-4909, doi:10.1175/JCLI-3247.1.
- Polavarapu, S., 2010: The stratospheric influence on the troposphere in the context of operational medium-range weather forecasts. Presentation at the SPARC Data Assimilation Workshop 2010, June 21-23 2010, Met Office, Exeter, UK, available from <http://www.atmosph.physics.utoronto.ca/SPARC/DA2010/Presentation.html>

- Scaife, A. A. and Knight, J. R., 2008: Ensemble simulations of the cold European winter of 2005-2006. *Q. J. R. Meteorol. Soc.*, **134**, 1647–1659. doi: 10.1002/qj.312.
- Stan, C., and D. M. Straus, 2009: Stratospheric predictability and sudden stratospheric warming events. *J. Geophys. Res.*, **114**, D12103, doi:10.1029/2008JD011277.
- Thompson, D.W.J., M.P. Baldwin, and J. M. Wallace, 2002: Stratospheric connection to Northern Hemisphere wintertime weather: Implications for prediction. *J. Climate*, **15**, 1421-1428.
- Thompson, D.W.J., J.C. Furtado, and T.G. Shepherd, 2006: On the Tropospheric Response to Anomalous Stratospheric Wave Drag and Radiative Heating. *J. Atmos. Sci.*, **63**, 2616-2629.
- Wittman, M. A. H., A.J. Charlton and L.M. Polvani, 2007: The effect of lower stratospheric shear on baroclinic instability. *J. Atmos. Sci.*, **64**, 479-496.